

# Experimental quantum key distribution with an untrusted source

Xiang Peng,<sup>1</sup> Hao Jiang,<sup>1</sup> Bingjie Xu,<sup>1</sup> Xiongfeng Ma,<sup>2</sup> and Hong Guo<sup>1,\*</sup>

<sup>1</sup>*CREAM Group, State Key Laboratory of Advanced Optical Communication Systems and Networks (Peking University) and Institute of Quantum Electronics,*

*School of Electronics Engineering and Computer Science,*

*Peking University, Beijing 100871, PR China*

<sup>2</sup>*Department of Physics and Astronomy,*

*Institute of Quantum Computing, University of Waterloo,*

*200 University Avenue West, Waterloo N2L 3G1, Ontario, Canada*

## Abstract

The photon statistics of a quantum key distribution (QKD) source is crucial for security analysis. In this paper, we propose a practical method, with only a beam splitter and photodetector involved, to monitor the photon statistics of a QKD source. By implementing in a Plug&Play QKD system, we show that the method is highly practical. The final secure key rate is 52 bit/s, comparing to 78 bit/s when the source is treated as a trusted source.

PACS numbers: 03.67.Dd

---

\*Electronic address: hongguo@pku.edu.cn

Quantum key distribution (QKD) can establish a secret key between two parties, Alice and Bob, by a quantum channel and an authenticated classical channel [1]. The unconditional security of QKD has been proven even when imperfect devices are used [2, 3].

A QKD system is composed of three parts: source, channel and detection. In the GLLP security analysis [2], the characteristics of these three parts are assumed to be fixed or measured and known to Alice and Bob. To guarantee the security of a real QKD experiment, one needs to carefully verify these assumptions.

The decoy state method [5, 6, 7] is proposed to characterize the properties of a QKD channel. Since a perfect single photon source is currently not available, an imperfect single photon source, such as a weak coherent state source, is used in real QKD setups. These imperfect single photon sources may contain some components that are not secure for QKD use, e.g., multi-photon state. When Alice and Bob are not able to monitor the channel properties, they have to pessimistically assume that all the losses and errors come from the single photon components. In this case, the QKD performance is very limited. Fortunately, with the decoy states, one can estimate the transmission efficiency of the single photon state accurately and improve the QKD performance dramatically. Note that in the security proof of decoy state QKD [6], the photon statistics of the source is assumed to be fixed and known to Alice and Bob. The main objective of the paper is to show how to monitor the photon source.

For the detection part, the squash model is assumed in the GLLP security analysis. With the squash model, one can assume that Eve, the eavesdropper, always sends a vacuum or qubit to Bob. In another word, Bob's measurement is performed on a vacuum or qubit. Recently, there are some works done in verifying the squash model [8, 9, 10].

The third part of the QKD system is the source, which is the main concern of this paper. Here, we consider the case that Eve has a full control of the photon source. That is, the source is untrusted. This is a crucial assumption in the security proof of some QKD schemes, such as the Plug&Play system [11]. Recently, the QKD with untrusted source is studied [12, 13]. By random sampling the photon source, the security is proved even when Eve controls the photon source [12]. This random sampling process requires a fast random switch and a perfect "intensity monitor". However, in reality, this is not practical.

In this paper, we replace the random switch with a passive beam splitter. An inefficient intensity monitor is used, which is modeled by a virtual beam splitter and an ideal detector.

The schematic diagram of the setup for Alice to monitor the photon source is shown in Fig. 1. In the following discussion,  $P_i$  with  $i = 1, \dots, 6$ , refers to position  $i$  in Fig. 1.

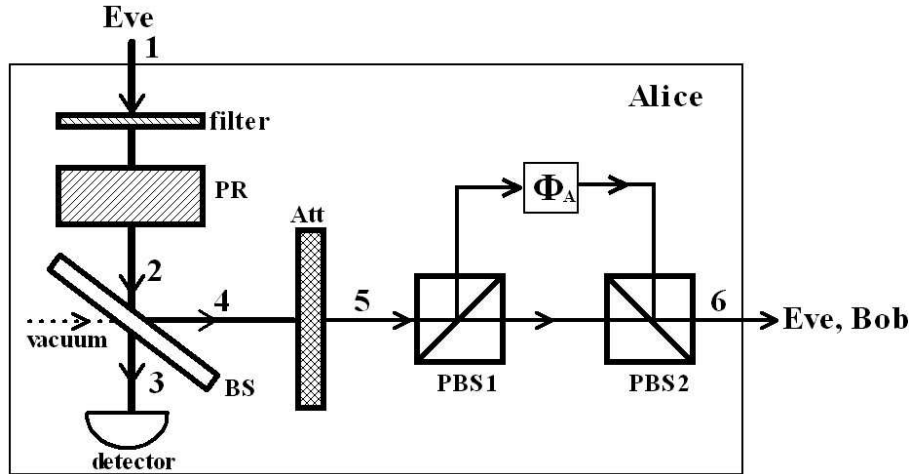


FIG. 1: A schematic diagram of the setup on Alice's side. The untrusted photon source, prepared at P1 by Eve, passes through a low-bandwidth filter and a phase randomizer (PR). Then a beam splitter (BS) (transmission:  $t_{bs}$ ) is used to separate it into two beams, 3 and 4. One beam goes to a photodetector (detection efficiency:  $t_D$ ) at P3 and the other is prepared for QKD at P4. An attenuator (Att) between P4 and P5 has the attenuation coefficient  $\eta_s$  ( $\eta_d$ ) for the signal (decoy) state. Two polarization beam splitters (PBS1 and PBS2) and a phase modulator ( $\Phi_A$ ) between P5 and P6 are used for phase encoding.

The experimental procedure goes as follows.

- (i) First, the untrusted photon source passes through a filter, which guarantees the state in single mode at P2. Then the global phase of the state is randomized by a phase randomizer (PR in Fig. 1). Thus, the state at P2 can be expressed as [6]

$$\rho_2 = \sum_{N=0}^{\infty} P_t(N) |N\rangle \langle N|, \quad (1)$$

where  $P_t(N)$  satisfies  $\sum_{N=0}^{\infty} P_t(N) = 1$  and  $|N\rangle$  is the number state.

- (ii) A small part ( $1 - t_{bs}$ ) of the beam at P2 will be reflected by the beam splitter (BS) to P4, and the rest of the beam will be transmitted to an inefficient photodetector at P3. The inefficient detector can be treated as another virtual beam splitter (transmission:  $t_D$ ) placed in front of an ideal detector. Thus, the photoelectron distribution  $D(m)$

measured at P3 is the Bernoulli transformation of the photon distribution  $P_t(N)$  at P2. On the other hand,  $P_t(N)$  can be inferred by the inverse Bernoulli transformation of  $D(m)$  [14]

$$\begin{aligned} D(m) &= B[P_t(N), \xi] = \sum_{N=m}^{\infty} P_t(N) \binom{N}{m} \xi^m (1-\xi)^{N-m}, \\ P_t(N) &= B^{-1}[D(m), \xi^{-1}] = \sum_{m=N}^{\infty} D(m) \binom{m}{N} \xi^{-N} (1-\xi^{-1})^{m-N}, \end{aligned} \quad (2)$$

where  $\xi = t_{bs}t_D$ . When  $\xi > 0.5$ , the  $P_t(N)$  distribution can be efficiently recovered from  $D(m)$  [15, 16].

- (iii) From P2 to P4 and P4 to P5, the state will be changed by the BS and an attenuator (Att in Fig. 1) with an attenuation coefficient  $1 - t_{bs}$  and  $\eta_s$  ( $\eta_d$ ) for signal state (decoy state), respectively. Thus, at P5, the photon number distribution  $P_s(i)$  for the signal state is  $B[P_t(N), \eta'_s]$  (see Eq. (2)) and  $P_d(i) = B[P_t(N), \eta'_d]$  for the decoy state, where  $\eta'_s = \eta_s(1 - t_{bs})$  and  $\eta'_d = \eta_d(1 - t_{bs})$ .

$D(m)$  can be measured directly from the experiment. Then  $P_t(N)$  can be calculated by Eq. (2). From  $P_t(N)$ , we can bound  $N \in [N_{min}, N_{max}]$  with a confidence  $(1 - \varepsilon)$ . Following [12], one can lower bound the gain  $Q_1^s$  ( $\underline{Q}_1^s$ ) and upper bound the error rate  $e_1^s$  ( $\overline{e}_1^s$ ) of the single photon state. The secure key rate can be written as [2, 12]

$$R = q \left[ -Q_s f(E_s) H_2(E_s) + (1 - \varepsilon) \underline{Q}_1^s (1 - H_2(\overline{e}_1^s)) \right], \quad (3)$$

where  $q$  is the basic reconciliation factor,  $Q_s$  and  $E_s$  are the overall gain and error rate of the signal state,  $f(E_s)H_2(E_s)$  is the leakage information in the error correction (normally,  $f(E_s) \geq 1$ ), and  $H_2(x) = -x \log_2 x - (1 - x) \log_2(1 - x)$  is the binary entropy function.

As shown in Fig. 2, we implement the aforementioned scheme in a standard Plug&Play QKD system. For applying the weak+vacuum decoy protocol, the experimental parameters are listed in Table I. The average photon numbers for the signal state and weak decoy state are  $\mu$  and  $\nu$ , respectively.  $N_\mu$ ,  $N_\nu$  and  $N_0$  are the pulse numbers for the signal, weak decoy and vacuum states, respectively. Note that 50 laser pulses are set as a pulse train whose period is 350  $\mu$ s. In Eq. (3), one can use  $q = 0.5F \cdot N_\mu / (N_\mu + N_\nu + N_0)$ , where  $F = 50\text{pulses}/350\mu\text{s}$  is determined by the burst mode of laser source. The temperature of laser diode is well-controlled for decreasing intensity fluctuations.

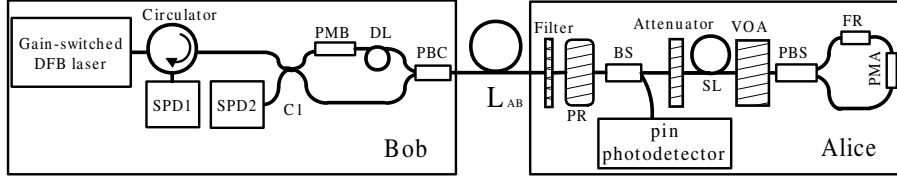


FIG. 2: Experimental setup for QKD system. A gain-switched distributed feedback (DFB) laser diode emits a pulse train of laser pulses [center wavelength: 1546.1 nm, pulse duration: 300 ps, pulse repetition rate: 1 MHz] which are polarized by the polarization maintaining (PM) fiber’s slow axis. The circulator and 50/50 coupler (C1) are polarization maintained. SPD1, SPD2: single photon detector; PBC/PBS: polarization beam combiner/splitter; PMA, PMB: phase modulator; DL: PM fiber;  $L_{AB}$ : 25 km single-mode fiber; SL: 5 km storage line; VOA: variable optical attenuator. A  $90^\circ$  Faraday rotator (FR), together with the PBS, plays the same role as a Faraday mirror. To implement the aforementioned scheme shown in Fig. 1, we use a filter (transparency window: 0.8 nm), phase randomizer (PR), 95/5 beam splitter (BS) and pin photodetector (detection efficiency  $t_D$ : 0.8).

$\mu$	$\nu$	$\xi$	$N_\mu$	$N_\nu$	$N_0$	$\eta'_s$	$\eta'_d$	$\eta_B$
0.48	0.06	0.76	61747531	23056601	5712393	$2.5 \times 10^{-8}$	$3.1 \times 10^{-9}$	0.04

TABLE I: The experimental parameters.  $\eta_B$  is the efficiency of Bob’s detection system.

To implement the scheme shown in Fig. 1, we use a beam splitter (BS) with  $t_{bs} = 0.95$  transmitting 95% of the laser beam to a pin photodiode. In total,  $\xi = t_{bs}t_D = 0.76$  of the incoming photon source is monitored by the photodiode. In the detection, an integrating capacitor is charged by the emitted photoelectrons and its voltage is proportional to the number of photoelectrons. The voltage signal is amplified, sent to a sampling oscilloscope (Tektronix MSO4104) and recorded. Before next photoelectron pulse arrives, due to the charge leakage, the capacitor is discharged.  $D(m)$  is experimentally measured and shown in Fig. 3.

The experimental data are shown in Table II.  $\langle m \rangle$  and  $\langle \Delta m^2 \rangle$  are the average number and variance of photoelectrons  $m$ , respectively. From Eq. (2), one can derive that  $\langle N \rangle = 1.914 \times 10^7$  and  $\langle \Delta N^2 \rangle = 1.063 \times 10^{11}$  for  $P_t(N)$ , in fact,  $\langle m \rangle = \xi \langle N \rangle$  and  $\langle \Delta m^2 \rangle = \xi(1 - \xi)\langle N \rangle + \xi^2 \langle \Delta N^2 \rangle$ . Fig. 3 shows that  $D(m)$  can be well fit as it is derived from the

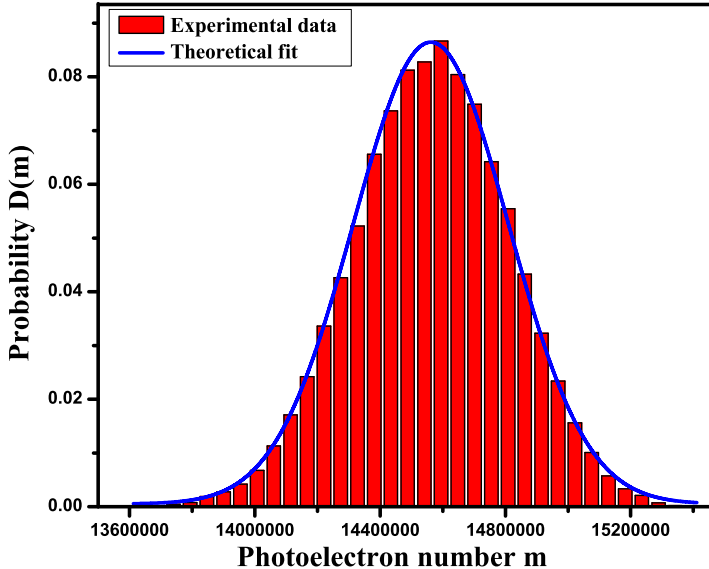


FIG. 3: (Color online) The photoelectron probability distribution  $D(m)$  with the experimental data shown as bars. The full curve represents the theoretical fit given that  $P_t(N)$  is Gaussian distribution.

Bernoulli transformation of a Gaussian distribution of  $P_t(N)$ .

$Q_s$	$Q_d$	$Q_0$	$E_s$	$E_0$	$\langle m \rangle$	$\langle \Delta m^2 \rangle$
$5.84 \times 10^{-3}$	$7.48 \times 10^{-4}$	$9.38 \times 10^{-5}$	2.1%	46.1%	$1.455 \times 10^7$	$6.14 \times 10^{10}$

TABLE II: The experimental results.

In the postprocessing, an improved ‘‘Cascade’’ protocol [17] is applied for the error correction and  $f(E_s)$  is estimated as 1.06 in Eq. (3). Based on the Gaussian distribution of  $P_t(N)$ ,  $N \in [N_{min}, N_{max}]$  with the confidence  $(1 - \varepsilon)$  are chosen as  $[1.751 \times 10^7, 2.077 \times 10^7]$  and  $(1 - 5.7 \times 10^{-7})$ , respectively. Then follow the analysis proposed in Ref. [12],  $Q_1^s$  and  $\overline{e_1^s}$  are  $2.58 \times 10^{-3}$  and 3.77%, and the secure key rate can be calculated as  $R \geq 52$  bit/s by Eq. (3). Note that with the same setup, the secure key rate is estimated as  $R \geq 78$  bit/s if the source is trusted.

We have following remarks:

1. Due to the computational complexity of the inverse Bernoulli transformation, see Eq. (2), we simply assume that  $P_t(N)$  follows the Gaussian distribution. As shown in Fig. 3, we deduce  $D(m)$  from  $P_t(N)$  and fit with experimental data. Note that how to calculate Eq. (2) in postprocessing efficiently is an interesting future topic.
2. In the experiment, the electronic noise can be deducted from the signal to enhance the estimation of  $D(m)$ . We use an oscilloscope to acquire data from the pin photodetector. The data transmission speed of the oscilloscope limits the speed of photon source monitoring. In the future, a high speed analog-to-digital circuit can be designed to replace the oscilloscope.
3. In the analysis, we assume that the photon source is single-mode after passing through an ideal filter. In the real experiment, the bandwidth of filter is not perfect. Thus, it is interesting to investigate how to analyze a multi-mode photon source for QKD in future.
4. Note that the statistical fluctuations from the finite data size [18, 19] and the accuracy of the estimation of  $D(m)$  are not considered in our security analysis, which are encouraged to be investigated in future.

In conclusion, a practical method to monitor the photon statistics of QKD source is proposed and is implemented in a real-life Plug&Play QKD system. We run the experiment around 20 minutes. The final secure key rate is 52 bit/s, comparing to 78 bit/s when the source is treated as a trusted source.

The fruitful discussions with H.-K. Lo, N. Lütkenhaus, B. Qi and Y. Zhao are greatly appreciated. We gratefully acknowledge T. Liu for his work on the efficiency of the error correction. This work is supported by the National Natural Science Foundation of China (Grant No. 10474004) and the National Hi-Tech Program. X. Ma acknowledges financial support from the University of Toronto and the NSERC Innovation Platform Quantum Works.

---

[1] C. H. Bennett and G. Brassard, in *Proceedings of IEEE International Conference on Computers, Systems, and Signal Processing* (IEEE, New York, Bangalore, India, 1984), pp. 175–179.

- [2] D. Gottesman, H.-K. Lo, N. Lütkenhaus, and J. Preskill, *Quant. Inf. Comput.* **4**, 325 (2004).
- [3] V. Scarani, H. Bechmann-Pasquinucci, N. J. Cerf, M. Dusek, N. Lütkenhaus, and M. Peev, arXiv: quant-ph/0802.4155 (2008).
- [4] H. K. Lo and Y. Zhao, arXiv: quant-ph/0803.2507 (2008).
- [5] W.-Y. Hwang, *Phys. Rev. Lett.* **91**, 057901 (2003).
- [6] H.-K. Lo, X. Ma, and K. Chen, *Phys. Rev. Lett.* **94**, 230504 (2005).
- [7] X.-B. Wang, *Phys. Rev. Lett.* **94**, 230503 (2005).
- [8] M. Koashi, arXiv:quant-ph/0609180 (2006).
- [9] T. Tsurumaru and K. Tamaki, arXiv: quant-ph/0803.4226 (2008).
- [10] N. J. Beaudry, T. Moroder, and N. Lütkenhaus, arXiv: quant-ph/0804.3082 (2008).
- [11] D. Stucki, N. Gisin, O. Guinnard, G. Ribordy, and H. Zbinden, *New J. of Phys.* **4**, 41 (2002).
- [12] Y. Zhao, B. Qi, and H. K. Lo, *Phys. Rev. A* **77**, 052327 (2008).
- [13] X. B. Wang, C. Z. Peng, J. Zhang, L. Yang, and J. W. Pan, *Phys. Rev. A* **77**, 042311 (2008).
- [14] C. T. Lee, *Phys. Rev. A* **48**, 2285 (1993).
- [15] T. Kiss, U. Herzog, and U. Leonhardt, *Phys. Rev. A* **52**, 2433 (1995).
- [16] U. Herzog, *Phys. Rev. A* **53**, 1245 (1996).
- [17] T. Sugimoto and K. Yamazaki, *IEICE Trans. Fundamentals* **E83-A**, 1987 (2000).
- [18] X. Ma, B. Qi, Y. Zhao, and H.-K. Lo, *Phys. Rev. A* **72**, 012326 (2005).
- [19] X.-B. Wang, *Phys. Rev. A* **72**, 012322 (2005).